# COMBINING HIGH SPATIAL RESOLUTION LIDAR DATA WITH AERIAL PHOTOGRAPHY TO AUTOMATE INDIVIDUAL TREE MEASUREMENTS

**Jun-Hak Lee**
**Joshua B. Fisher**
Department of Environmental Science, Policy and Management,
University of California, Berkeley,
137 Mulford Hall,
Berkeley, CA 94720

## ABSTRACT

Detailed forest inventory information is critically required for many ecological applications as well as for forest management. However, traditional field measurements, which are labor intensive and time consuming, can provide only a very limited amount of information for large forest areas so that extrapolated estimation of forest characteristics tends to have large errors. With the help of new technologies, we have high spatial resolution remotely sensed data. Since every sensor has its own strengths and weaknesses, one sensor cannot provide all the information we want to acquire. While both small foot print LiDAR data and large scale aerial photographs have the ability to extract individual tree level of biophysical characteristics in large forests, the former do not have spectral information and the latter have problems with automatic extraction of height information because of distortion and heterogeneous tree shapes. In this study we combine LiDAR data and aerial photographs to automate individual tree measurements of South Fork Eel forests in Northern California. First, we generate Canopy Height Model (CHM) from Digital Terrain Model (DTM) and Crown Surface Model (CSM) detect individual tree top locations and tree heights with LiDAR data using morphological analysis. Next, we obtain tree top locations from aerial photography with morphological analysis. Finally, we conducted an accuracy assessment for both LiDAR data and aerial photography to evaluate performance of our methods. The morphological analysis detected tree top locations with a User's and Producer's accuracy of 85% and 51% for LiDAR and 55% and 43% for aerial photography.

## INTRODUCTION

Forests provide economic goods such as timber, food, fuel, and fiber in addition to ecological services such as clean water and air, soil stabilization, habitat conservation, and protection of biodiversity. However, forested areas have rapidly decreased because of the demand for resources and land use by population growth (Franklin, 2001). In addition, the reduction of forested areas, in combination with increasing fossil fuel consumption, has been altering global climate. Forest disturbances such as deforestation, fire, disease, and invasive species have become more severe because of climate change, which, in turn, weaken and threaten the sustainability of forest ecosystems (USDA Forest Service, 2003). To reduce these problems and sustain benefits from forests, we need proper decisions for the use and preservation of forests. In order to achieve balance between use and preservation, detailed and spatially continuous forest information (individual tree level) is required for large forested areas because forest ecosystem processes cannot be described correctly with extrapolated estimation for the entire forest based on a small portion of forest field measurements–a few tree measurements cannot reflect a heterogeneous and complex forest ecosystem. Recently, with sensing and computing technological development, we can extract individual tree level information for large forest areas from high spatial resolution remotely sensed data, such as Light Detection and Ranging (LiDAR) and digital aerial photography.

Because LiDAR provides horizontal and vertical information at high spatial resolutions, individual tree attributes can be extracted from forests (Lim et al., 2003; Hyyppä *et al.*, 2004). Many researchers have used LiDAR to delineate or isolate individual trees with good success (Hyyppä *et al.*, 2001; Andersen et al., 2002; Persson *et al.*, 2002; Brandtberg *et al.*, 2003; Morsdorf et al., 2003; Popescu *et al.*, 2003; Chen et al. in press). Nonetheless, LiDAR has limited spectral information, which is needed to extract species or health information from the trees. Further, because LiDAR is so new, the spatial and historical archives are limited (Baltsavias, 1999).

Aerial photography has also been used to isolate individual trees from forests, either manually or automated. With these methods many forest biophysical parameters, such as tree height, crown diameter, stem diameter, and

stem volume can be measured as accurately as field measurements (Hyyppa et al., 2001; Culvenor, 2002; Persson et al. 2002). Additionally, we have an extensive historical record of aerial photos over the past 6 decades, thus making retrospective analyses possible (Brandtberg, 1999). Even though the manual stereo photogrammetric method is much easier to apply than are field measurements (Gong et al., 2002), this method could be vulnerable to subjective and systematic errors by the operators (Wang et al., 2004). Therefore, an accurate automated process is essential for individual tree recognition. Unlike with LiDAR, however, it is difficult to acquire accurate tree heights with aerial photography because forest floors are barely seen in dense forest areas (Popescu et al., 2002). Although many studies have attempted to automate individual tree delineation with aerial photography, limited success has been gained because heterogeneous colors and the discontinuities in tree foliage create complications in matching pixels in an overlapping photos (images) needed to create a 3D model (Sheng et al., 2003).

If aerial photography and LiDAR can be combined, then we can delineate individual trees (LiDAR) and derive biophysical parameters (aerial photography) at the tree level. We can extract individual tree biophysical characteristics automatically and accurately because the information extracted from each data source can serve as auxiliary information for the other one (Popescu et al., 2004). For example, the tree locations and height from LiDAR can be used for finding tree tops from aerial photos to match image pairs (Larsen and Rudemo, 2004). On the other hand, spectral values of aerial photos can be used to classify land cover type and this information and can serve to distinguish shrubs and bare soil. In order to combine two or more data sources, matching methods should be elaborated. Dominant tree tops could be used as Ground Control Points (GCPs) to co-register different data sources because tree tops are relatively accurate and easy to detect in both kinds of data source.

There have been several attempts to measure forest biophysical characteristics from fusing LiDAR and aerial photography in high spatial resolution, but the major problem that continues to arise is image matching, particularly when automated (Leckie et al., 2003, McCombs et al., 2003, Suarez et al., 2005). St-Onge et al. (2004) used LiDAR for topographic elevation to measure tree height with aerial photos. Popescu et al. (2004) use high spatial resolution CASI imagery to extract land cover information when using LiDAR to estimate tree height. Leckie et al (2003) extracted individual tree information from LiDAR and multispectral imagery but matching between two data sets was not performed. While there has been much research, it is still not easy to combine two data sources at the individual tree level, so the benefit of high spatial resolutions cannot be maintained.

The objective of our study is combining high spatial resolution LiDAR data and aerial photography to extract individual tree information. More specific aims are: 1) Detect individual tree top location from LiDAR data and aerial photography using morphological operation procedures 2) Evaluate of accuracy of tree top detection performance by data sources (LiDAR and aerial photography).

## MATERIALS AND METHODS

### Study Site

This study was conducted at Angelo Coast Range Reserve, part of the University of California Natural Reserve System on South Fork of Eel River in Mendocino County, CA. The Angelo Coast Range Reserve is composed of old conifer forest, dominated by *Pseudotsuga menziesii* (Douglas Fir) and *Sequoia sempervirens* (Redwood) forest (Kotanen, 2004). Elevation ranges from 378 m to 1290 m. Average temperatures range from 16ºC to 31ºC with annual average precipitation of 216 cm/yr (UC Natural Reserve System, http://nrs.ucop.edu/Angelo.htm, 02/12/06). We studied a 4 $km^2$ subset of the larger 180 $km^2$ of the South Fork Eel river watershed for which LiDAR and aerial photos were acquired by the National Center for Earth-surface Dynamics.

### Data

Both the LiDAR data and aerial photography were acquired simultaneously on the same plane on June 2004. LiDAR data were recorded by the Airborne Laser Swath Mapping (ALSM) system mounted on a Cessna 337 airplane. The ALSM system is comprised of an Optech Inc. model 1233 Airborne Laser Terrain Mapper (ALTM) unit, Inertial Measurement Unit (IMU) and Differential Global Positioning System (DGPS). The laser pulse frequency is 33 kHz and swath width is 20 degrees per half angle. The datasets include the first and last pulses for x, y, z coordinates, intensity value, and GPS time. The system acquires 2-3 pulses per 1 $m^2$ so that the spatial resolution is generally less than 1 m with vertical accuracy of 5-10 cm and horizontal accuracy of 15-20 cm.

Digital aerial photography were recorded by an optical 3-Charge-Coupled Device (CCD) digital multispectral camera (Redlake MASD Inc., model MS4100). The resolution is 1920(H) x 1080(V) for 2 million pixels with 3 visible bands (R,G,B). The 28mm focal length lens has a 15 cm x 15 cm spatial resolution at 550 m flight height.

## LiDAR Analysis

Because ground elevation information directly acquired from LiDAR points includes terrain elevation as well, a ground digital elevation model must be generated to separate tree crown height from the LiDAR point data set (Popescu et al., 2002). Not all the LiDAR points can penetrate the canopy and give terrain elevation information, however, so appropriate filtering procedures must be used to select points back-scattered from the terrain to generate an accurate Digital Terrain Model (Suarez et al., 2005). Sithole and Vosselman (2004) review a suite of filtering algorithms to extract points from the ground—slope-based, block-minimum, surface-based, and clustering/segmentation—each with their own strengths and limitations. We applied a multiple-method approach to remove non-ground objects and for a robust digital terrain model from LiDAR.

First, we created a $1m^2$ grid from the last return of LiDAR points. Within each cell, a minimum elevation point was selected to generate a digital elevation model using a linear interpolation method. Cell size was decided based on the density of LiDAR points for the area (3.1 points per $m^2$) so that each cell on average contained 2-3 points. Next, we used the surface-based iterative morphological filtering method (Chen et al., in press) as the opening operation to remove returned points from non-ground objects (Figure 1-A). Although this method worked well for Chen et al. (in press) for their flat, sparse canopy, urban and rural study areas, the method was problematic for our steep, dense canopy site because our LiDAR data set did not include as many returned points. For these reasons, the morphological filtering method resulted in mostly flat ground surface (Figure 1-B), which is not close to the real ground surface, though the points returned from the above ground trees were successfully removed. We used the DTM generated from the morphological filtering method, but we apply more steps to correct the DTM. Using the grid surface that we created with morphological filtering, LiDAR points were divided into two groups, returned from ground points and non-ground points. We used linear interpolation to generate the new DTM with ground returned points. However, there were still a few misclassified points, which made a small bumpy surface. To remove these points from ground returned points, the maximum elevation difference from terrain points and 5 x 5 neighbor cells were calculated with a threshold if the maximum difference was larger than 5 m, the points were classified as non-ground points. Finally, digital terrain model was generated using cubic interpolation with the points classified as ground return (Figure 1-C).

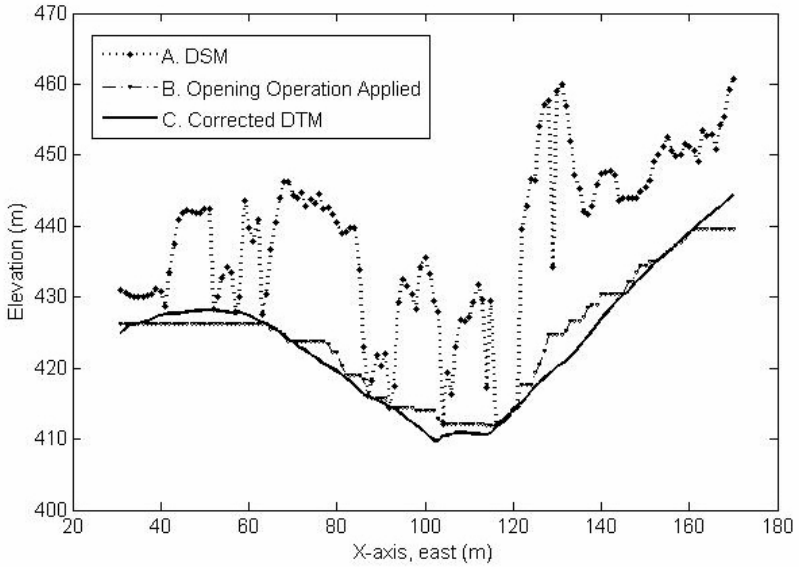


**Figure 1**. Example of generating corrected DTM from DSM. (A) DSM from last return points, (B) DTM with opening operation with flat areas, (C) corrected DTM

The Canopy Height Model was obtained by subtracting canopy surface (generated with canopy hit LiDAR points) from the DTM (Figure 2). The canopy surface model grid was created with the same cell size (1m x 1m) that was used for the DTM. In contrast to the DTM, which used minimum elevation points, the Canopy Surface Model (CSM) used the maximum elevation points from both first and last returns. Linear interpolation then generated the canopy surface model (Figure 3).

Tree tops were delineated with the morphological top-hat transformation, which can extract the apex of individual tree crowns (Anderson, 2001). The opening process depresses hat-shaped objects smaller than structural element (i.e. disk with certain size of radius) from canopy height model, so that if we subtract the result of the morphological opening operation from the original canopy height model, only the tips of individual trees remain. Because this method can extract not only the apex of an individual tree but also a pseudo-apex (such as large branch), selecting the proper size for the structural elements is critical. In our research, radius (1.5m) was selected iteratively with different sizes of structural elements.

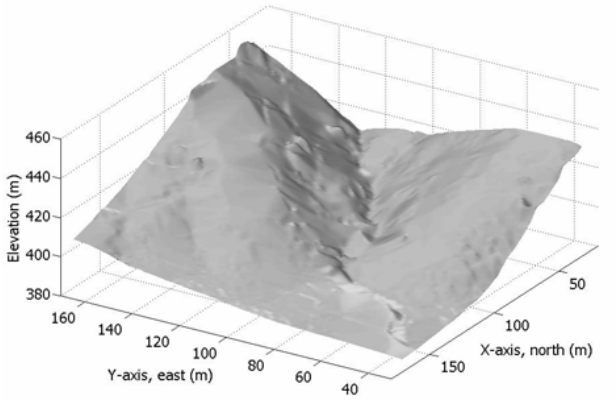


**Figure 2**. DTM from LiDAR data.

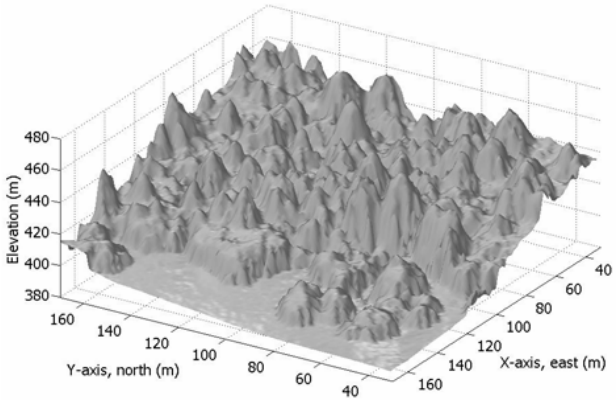


**Figure 3**. DSM from first return.

## Aerial Photography Analysis

Preprocessing is necessary to prepare a suitable image for individual tree delineation (Gougeon and Leckie 2003). First, the image is geometrically corrected with 1st order polynomial functions (Toutin, 2004). This geometric correction is performed only for visual interpretation of aerial photography with LiDAR data. During the process, the spatial resolution of images changed from 15 cm x 15 cm to match the 1m x 1m for the LiDAR data. We selected the green band for tree top delineation because it is often used in forest inventories (Gougeon and Leckie, 2003) and we did not have near-infrared wavelengths, which are also used frequently in forest inventories. We used a Gaussian filter for smoothing to remove noise and outlying variance in the images (Pouliot and King, 2005; Pitkänen, 2001).

For an individual tree, the tree top is the brightest part because the peak is more likely to be directly illuminated from different sun angles than is the edge parts for the convex shape of a tree; adjacent trees will shade the edges of their neighbor (Wulder, 2003). Thus, reflectance value can represent relative height within an individual tree. The same method as described for extracting individual tree tops from CHM with the LiDAR data was applied to extract tops of individual trees from aerial photography with reflectance values. We applied the same size of structural elements to acquire as similar a match as possible. For the accuracy assessment of tree top detection performance, reference data were collected from LiDAR data and aerial photography with visual interpretation.

## Accuracy Assessment

For the accuracy assessment of tree top detection performance, reference data were collected from LiDAR data and aerial photography with visual interpretation. Using both CHM from LiDAR and aerial photographs the locations of individual tree top were manually extracted. Because we extract the tree tops from the same area for both LiDAR and aerial photography all trees used for reference in our study are the same (99 trees). However, the image from aerial photography is not ortho-rectified so that we cannot use one reference data for the other. As a result, the reference locations for each tree were depicted separately for each data sources.

In order to assess the accuracy detected tree top locations matched to nearest tree top locations from reference data and if the distance between detect by our method and reference points are less than 2m, it is concerned as “correct”. User's accuracy (measure of omission errors) is the number of correct points divided by the total number of points detected by algorithm and Producer’s accuracy (measure of commission errors) is the number the number of correct points divided by the total number of points in the reference points (Andersen et al. 2001).

## RESULTS

Model accuracy was determined from a combination of two complementary factors: 1) number of reference (actual) trees for which there was no nearby predicted tree; and 2) number of predicted trees for which there was no nearby reference tree. "Nearby" is defined as predicted crown center within 2 m of actual crown center, though this value should be determined by the morphology of the vegetation (larger crowns should warrant a larger allowable matching error). The first factor is an indication of missed trees, or Producer's accuracy, which is the total number of "hits"—or reference trees to which there were nearby predicted trees—divided by the total number of "hits" possible. Our model driven by LiDAR hit 51 out of a total of 99 reference trees (Figure 6). The model driven by aerial photography hit a similar 54 of those trees. The second factor is an indication of false positives, or User's accuracy, which is 100% minus the percent of trees predicted, but there were no nearby reference trees. Our model driven by LiDAR gave only 9 false positives (60 predicted, but only 51 matches). The model driven by aerial photography (Figure 7) gave 58 false positives (112 predicted, but only 54 matches). The model driven by LiDAR was clearly more accurate than as driven by aerial photography (Table 1).

**Table 1. User's versus Producer's accuracy for LiDAR and aerial photography**

| | User's Accuracy | Producer's Accuracy |
|---|---|---|
| LiDAR | 85% | 52% |
| Aerial Photography | 55% | 43% |

Because LiDAR sensors measure the physical distance to the objects, shape information is revealed in the 3D coordinates of points. The peaks of tall objects tend to be the brightest points as well, which is captured by aerial photography, though this is not a direct measure of object height. Using LiDAR only, the accuracy of individual tree detection increases as the tree increases in height (Figure 4). Still, an accuracy plateau emerges at 60% for trees greater than 20 m. Further, at only 60% accuracy, we still missed three out of six tall trees (> 35 m). Because large trees often have a less sharp apex compared to smaller trees, the morphological opening filter missed tree tops from large trees.

Additionally, individual tree detection accuracy increases with increased spacing distance between trees (Figure 5). Accuracy increases by almost five times as spacing increases from 4 m to 6 m. A slight rise is evident in accuracy as spacing increases from 6 to 10 m, then another large jump in accuracy for spacing greater than 10 m.

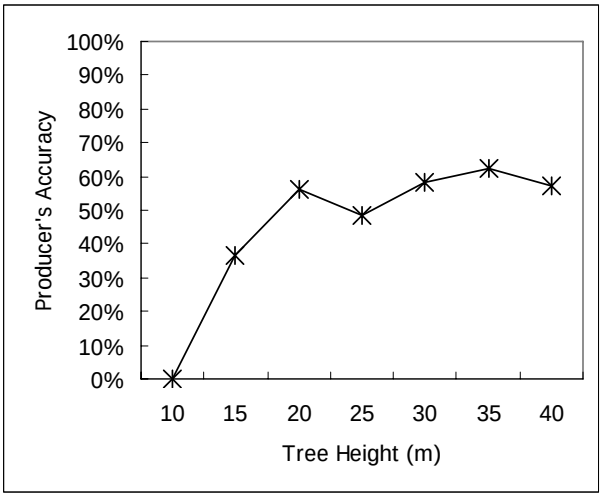


**Figure 4**. Individual tree detection increases with tree height, then plateaus.

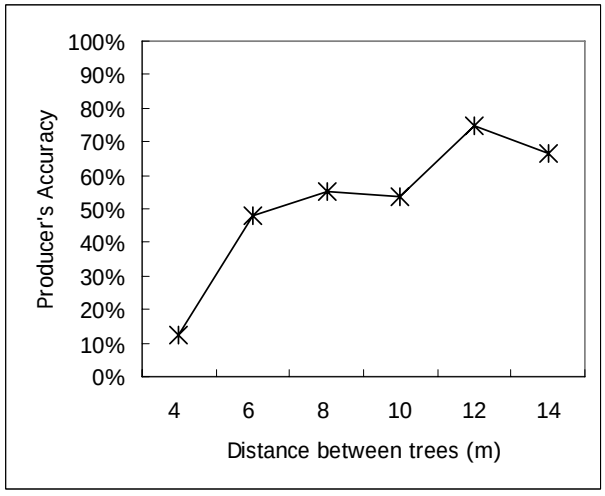


**Figure 5**. Individual tree detection accuracy increases with spacing distance between trees.

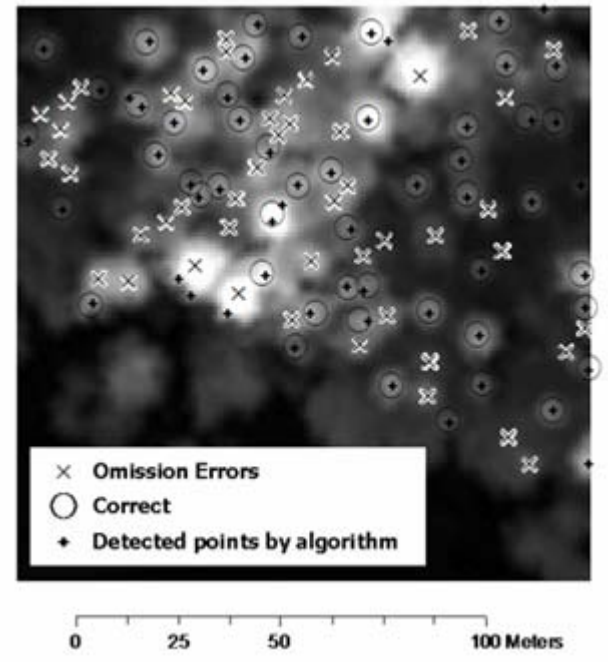


**Figure 6**. Tree tops extracted from LiDAR data ("O" and "X" represent reference tree tops and "+" represent detected tree tops by algorithm)

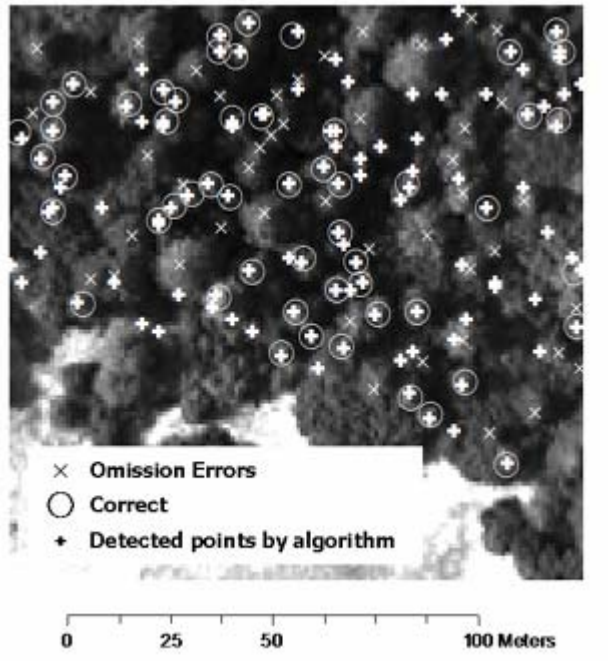


**Figure 7**. Tree tops extracted from aerial photography ("O" and "X" represent reference tree tops and "+" represent detected tree tops by algorithm)

## DISCUSSION

Tree top detection from LiDAR data with morphological filtering resulted in small commission error (15%) and large omission error (48.5%). Small commission error means that detected tree top locations have high accuracy but large omission error showed many tree top locations missed using our method. Anderson et al. (2001) reported on the importance of bin size (cell size) and parameters of the morphological operations (size of structural element) and parameters have different performance as the size of trees. In our study, detection accuracy is increased as tree size and distance from nearest neighbor tree are enlarged but there are some missing trees even for tall trees. We assume that the lack of accuracy of detection for both small and tall trees is due to fixed parameters for the entire study site. Chen et al. (in press) applied a variable window size for local maxima to detect tree tops from LiDAR data based on tree height and Popescu and Waynne (2004) used the relationship between tree height and crown size to delineate individual trees. Hence, for future study, we plan to include the relationship between tree height, which can be estimated by the difference between CSM and DSM, and crown radius. In addition, other forest biological characteristics like crown radius, crown area or leaf area for each tree, and even topographic characteristics such as the index of productivity of soil, can be included for the individual tree delineation procedures.

Although we used the same method for LiDAR data and aerial photography, the detection performances and the results are different between the two data sources and the performance of morphological operation for aerial photography was not good enough for detecting tree tops. Therefore, a more accurate method would be to partition the tree top detecting method based on the characteristics of data sources. Wulder (2003) divided automated crown delineation methods using high resolution optical sensor data into 3 groups: bottom-up algorithms (valley following and directional texture analysis), top-down algorithms (multiscale edge segments, threshold-based spatial clustering, and vision expert system), and template-matching algorithms. For future study, we can apply different methods to our study site and select the best methods to obtain individual tree top location information with allowable accuracy, which can be used to match the tree top points from aerial photography to those from LiDAR data. As mentioned above, tree top location detecting can be improved if biological characteristics of trees are included during evaluation to find individual tree tops from aerial photography as well.

The LiDAR data, which were originally created as 3D-georefereneced points, can be used as a reference to register aerial photography. But, because aerial photography transforms the 3D surface to a 2D plane, there are many local geometric distortions, especially for high spatial resolution images, caused by various surface heights,

and low effects of pitch, roll, and yaw (Devereux, 1990). The local transformation model, which uses several transformation equations by partitioning the interest region, is more appropriate for our case than is global transformation, which uses only one equation for the whole area and cannot justify local variations (Habib and Alruzoua, 2004). The largest concern for using local transformation, however, is that the model requires a large number of control points, which are difficult to extract both automated and manually (Liu et al., in press). We can extract tree top points with automated methods from both LiDAR and aerial images to be used as control points for the local transformation model. The tree top locations from the aerial images have different radial displacement due to tree height and lack of ortho-rectification, however. To solve this problem, tree top locations in aerial photography can be estimated from those of the LiDAR data set with height information from CSM. Because tree top locations from LiDAR already have georeferenced 3D coordinates, we could estimate radial displacement for individual tree tops and calculate tree top locations in the images.

We generated referenced tree top locations with CHM and aerial photography. Even though we visually crosschecked CHM and aerial photography for each other to remove the errors, there could be some errors in our reference tree top locations because it is possible that we missed some small trees with both CHM and aerial photography. Although omission error from both LiDAR and aerial photography is not cause a big problem for the matching purpose, it could be problematic for forest inventory or forest ecology applications. Thus, we must collect reference data from field measurements and compare them to visual interpretation from remotely sensed data.

The accuracy assessment method, which uses only nearest neighbor distance, can be improved. One of the biggest problems in using nearest neighbor distance to calculate accuracy is that the accuracy can vary based on the radius that is assigned. In addition, the nearest neighbor method can match incorrectly when the actual matching point is further than another closer neighbor point. To overcome this problem, the area of individual tree crowns can be added to decide the matching accuracy. Nelson et al (2005) converted tree locations to Voronoi Polygons (VP) to determine matching accuracy and Chen et al. (in press) applied Absolute Accuracy for Tree Isolation (AATI), which use overlapping area between crown boundaries.

We evaluated the possibility of combining high spatial resolution LiDAR data and aerial photography with automated detection of tree top locations using the morphological operation. The performance of tree top detection showed little commission error but large omission error for LiDAR data due to the static morphological operation parameters for all tree sizes. We found that aerial photography did not provide similar results to LiDAR data given the exact same method. Thus, we need to elaborate to develop more robust tree top detection methods, which can provide us enough detecting accuracy that we can apply a local transform model to combine LiDAR and aerial photography with detected tree top locations for extracting individual tree level information from large forest areas.

## ACKNOWLEDGEMENTS

We wish to thank to Gregory S. Biging, Peng Gong, William E. Dietrich, Qi Chen, Desheng Liu, Collin Bode, Dino Bellugi, Seong-Woo Jeon, and Woo-Kyun Lee for assistance and support in this research. Our gratitude also goes to National Center of Airborne Laser Mapping (NCALM) for providing LiDAR and aerial photography for the research purpose.

## REFERNCES

Andersen, H., S.E. Reutebusch, and G.F. Schreuder (2001). Automated individual tree measurement through morphological analysis of a LIDAR-based canopy surface model. Proceedings of *the First International Precision Forestry Cooperative Symposium*, University of Washington, Seattle, USA, June 17-20, pp. 11-22.

Andersen, H-E, Reutebuch, S., Schreuder, G. (2002). Bayesian Object Recognition for the Analysis of Complex Forest Scenes in Airborne Laser Scanner Data. *International Archives of the Photogrammetry, Remote Sensing and Spatial Information Sciences*, 34:35-41.

Baltsavias, E.P. (1999). Airborne laser scanning: existing systems and firms and other resources. *ISPRS Journal of Photogrammetry & Remote Sensing*, 54:164–198

Brandtberg, T. (1999). Remote Sensing for Forestry Applications—A Historical Retrospect. Available online at http://www.dai.ed.ac.uk/CVonline/LOCAL_COPIES/BRANDTBERG/UK.html (last accessed 2 Feb 2006).

Brandtberg, T., T.A. Warner, R.E. Landenberger, and J.B. McGraw. (2003). Detection and analysis of individual leaf-off tree crowns in small footprint, high sampling density lidar data from eastern deciduous forest in North America. *Remote Sensing of Environment*, 85:290-303

Chen, Q., P. Gong, D. Baldocchi, and G. Xie. Filtering airborne laser scanning data with morphological methods, *Photogrammetric Engineering and Remote Sensing* (in press)

Culvenor, D.S. (2002) TIDA: an algorithm for the delineation of tree crowns in high spatial resolution remotely sensed imagery. *Computers and Geosciences*, 28:33–44.

Liu, D., P. Gong, M. Kelly, and Q. Guo, Automatic Registration of Airborne Images with Complex Local Distortion. *Photogrammetric Engineering and Remote Sensing* (in press)

Devereux, B.J., R.M. Fuller, L. Carter, and R.J. Parsell (1990). Geometric correction of airborne scanner imagery by matching delaunay triangles, *International Journal of Remote Sensing*, 11(12): 2237-2251.

Franklin, S.E. (2001). *Remote sensing for sustainable forest management*. Lewis, Boca Raton, Fla.

Gong, P., Y. Sheng, and G.S. Biging (2002). 3d model-based tree measurement from high-resolution aerial imagery, *Photogrammetric Engineering & Remote Sensing*, 68(11):1203–1212.

Gougeon, F., and Leckie, D. (2003) Forest information extraction from high spatial resolution images using an individual tree crown approach. Information report BC-X-396, Natural Resources Canada, Canadian Forest Service, Pacific Forestry Centre, 26 p.

Habib, A.F. and Alruzouq R.I. (2004) Line-based modified iterated Hough transform for automatic registration of multi-source imagery. *Photogrammetric Record*,19(105): 5-20

Hyyppä, J., H. Hyyppä, P. Litkey, X. Yu, H. Haggrén, P. Rönnholm, U. Pyysalo, J. Pitkänen, and M. Maltamo (2004). Algorithms and methods of airborne laser scanning for forest measurements. *International Conference Natscan - "Laser-Scanners for Forest and Landscape Assessment - Instruments, Processing Methods and Applications"* Keynote presentation, Freiburg, 4-6. October 2004.

Hyyppä, J., O. Kelle, M. Lehikoinen, & M. Inkinen (2001). A segmentation-based method to retrieve stem volume estimates from 3-D tree height models produced by laser scanners. *IEEE Transactions on Geoscience and Remote Sensing*, 39:969-975.

Kotanen, Peter M. (2004). Revegetation following soil disturbance and invasion in a Californian meadow: a 10-year history of recovery. *Biological Invasions*, 6: 245–254

Larsen, M. and M. Rudemo (2004). Approximate Bayesian estimation of a 3D point pattern from multiple views. *Pattern Recognition Letters*, 25(12):1359-1368.

Leckie D., F. Gougeon, D. Hill, R. Quinn, L. Armstrong, & R. Shreenan. (2003). Combined high-density lidar and multispectral imagery for individual tree crown analysis, *Canadian Journal of Remote Sensing*, 29(5):1-17.

Lim K, P. Treitz, M. Wulder, B. St-Onge, and M. Flood (2003). LiDAR remote sensing of forest structure. *Progress in Physical Geography*, 27(1): 88–106

McCombs, J.W., S.D. Roberts, and D.L. Evans (2003). Influence offusing LiDAR and multispectral imagery on remotely sensed estimates of stand density and mean tree height. *Forest Science*. 49:457–466.

Morsdorf, F., E. Meier, B. Allgöwer, and D. Nüesch, (2003). Clustering in airborne laser scanning raw data for segmentation of single trees. *International Archives of the Photogrammetry, Remote Sensing and Spatial Information Sciences*, Vol 34, part 3/W13, pp 27-33.

Nelsona, T., B. Bootsa, and M.A. Wulder (2005). Techniques for accuracy assessment of tree locations extracted from remotely sensed imagery. *Journal of Environmental Management*, 74:265–271

Persson., Å, J. Holmgren, U. Söderman (2002). Detecting and measuring individual trees using an airborne laser scanner. *Photogrammetric Engineering and Remote Sensing*, 68(9):925-932.

Pitkänen, J. (2001). Individual tree detection in digital aerial images by combining locally adaptive binarization and local maxima methods. *Canadian Journal of Forest Research*, 31(5):832–844.

Popescu, S. C., R. H. Wynne, and R. F. Nelson. (2003). Measuring individual tree crown diameter with lidar and assessing its influence on estimating forest volume and biomass, *Canadian Journal of Remote Sensing*, 29:564-577

Popescu, S.C., R.H. Wynne, and J.A. Scrivani (2004). Fusion of small-footprint lidar and multispectral data to estimate plot-level volume and biomass in deciduous and pine forests in Virginia, USA. *Forest Science*, 50(4):551-565

Popescu, S.C., R.H. Wynne, and R.F. Nelson (2002). Estimating plot-level tree heights with lidar: Local filtering with a canopy-height based variable window size. *Computers and Electronics in Agriculture*, 37: 71-95

Pouliot, D. A. and King, D. J. (2005) Approaches for optimal automated individual tree crown detection in young regenerating coniferous forests. *Canadian Journal of Remote Sensing*, 31: 256–267.

Sheng, Y, P. Gong and G.S. Biging (2003). Model-based conifer canopy surface reconstruction from photographic imagery: overcoming the occlusion, foreshortening, and edge effects. *Photogrammetric Engineering & Remote Sensing*, 69(3):249-258

Soille, G. and G. Vosselman (2004). Experimental Comparison of Filter Algorithms for Bare Earth Extraction from Airborne Laser Scanning Point Clouds, *ISPRS Journal of Photogrammetry and Remote Sensing*, 59(1-2):85-101

St-Onge, B., J. Jumelet, M. Cobello, and C. Véga (2004). Measuring individual tree height using a combination of stereophotogrammetry and lidar. *Canadian Journal of Forest Resources*, 34(10):2122-2130

Suárez, J., C. Ontiveros, S. Smith, and S. Snape (2005). The Use of Airborne LiDAR and Aerial Photography in the Estimation of Individual Tree Heights in Forestry. *Computers & Geosciences*, 31(2):253-262

UC Natural Reserve System, Angelo Coast Range Reserve. Available online at http://nrs.ucop.edu/Angelo.htm (last accessed 12 Feb 2006)

USDA Forest Service (2003). National report on sustainable forests-2003. Washington, DC. Available online at www2.srs.fs.fed.us/2003/2003.htm (last accessed 6 January 2006).

Wang, L., P. Gong, G.S. Biging. (2004) Individual Tree-Crown Delineation and Treetop Detection in High Spatial-Resolution Aerial Imagery. *Photogrammetric Engineering & Remote Sensing*, 70: 351–357.

Wulder M.A. and S.E. Franklin (2003). *Remote sensing of forest environments. Concepts and casestudies*. Kluwer Academic Publishers, Boston.